ISSN 1001-0742
CN 11-2629/X

2012
Volume 24
Number 6

JOURNAL OF

ENVIRONMENTAL SCIENCES

ELSEVIER
Science Press

Sponsored by
Research Center for Eco-Environmental Sciences
Chinese Academy of Sciences

JOURNAL OF ENVIRONMENTAL SCIENCES

(http://www.jesc.ac.cn)

Aims and scope

Journal of Environmental Sciences is an international academic journal supervised by Research Center for Eco-Environmental Sciences, Chinese Academy of Sciences. The journal publishes original, peer-reviewed innovative research and valuable findings in environmental sciences. The types of articles published are research article, critical review, rapid communications, and special issues.

The scope of the journal embraces the treatment processes for natural groundwater, municipal, agricultural and industrial water and wastewaters; physical and chemical methods for limitation of pollutants emission into the atmospheric environment; chemical and biological and phytoremediation of contaminated soil; fate and transport of pollutants in environments; toxicological effects of terrorist chemical release on the natural environment and human health; development of environmental catalysts and materials.

For subscription to electronic edition

Elsevier is responsible for subscription of the journal. Please subscribe to the journal via http://www.elsevier.com/locate/jes.

For subscription to print edition

China: Please contact the customer service, Science Press, 16 Donghuangchenggen North Street, Beijing 100717, China. Tel: +86-10-64017032; E-mail: journal@mail.sciencep.com, or the local post office throughout China (domestic postcode: 2-580).

Outside China: Please order the journal from the Elsevier Customer Service Department at the Regional Sales Office nearest you.

Submission declaration

Submission of an article implies that the work described has not been published previously (except in the form of an abstract or as part of a published lecture or academic thesis), that it is not under consideration for publication elsewhere. The submission should be approved by all authors and tacitly or explicitly by the responsible authorities where the work was carried out. If the manuscript accepted, it will not be published elsewhere in the same form, in English or in any other language, including electronically without the written consent of the copyright-holder.

Submission declaration

Submission of the work described has not been published previously (except in the form of an abstract or as part of a published lecture or academic thesis), that it is not under consideration for publication elsewhere. The publication should be approved by all authors and tacitly or explicitly by the responsible authorities where the work was carried out. If the manuscript accepted, it will not be published elsewhere in the same form, in English or in any other language, including electronically without the written consent of the copyright-holder.

Editorial

Authors should submit manuscript online at http://www.jesc.ac.cn. In case of queries, please contact editorial office, Tel: +86-10-62920553, E-mail: jesc@263.net, jesc@rcees.ac.cn. Instruction to authors is available at http://www.jesc.ac.cn.

Copyright

ISSN 1001–0742 **Journal of Environmental Sciences** Vol. 24 No. 6 2012

CONTENTS

Serial parameter: CN 11-2629/X*1989*m*188*en*P*22*2012-6

Available online at www.sciencedirect.com
ScienceDirect
Journal of Environmental Sciences 2012, 24(6) 1117–1124
JOURNAL OF ENVIRONMENTAL SCIENCES
ISSN 1001-0742
CN 11-2629/X
www.jesc.ac.cn

Preparation of birnessite-supported Pt nanoparticles and their application in catalytic oxidation of formaldehyde

Linlin Liu[1,2], Hua Tian[1], Junhui He[1,*], Donghui Wang[3], Qiaowen Yang[2]

1. Functional Nanomaterials Laboratory and Key Laboratory of Photochemical Conversion and Optoelectronic Materials, Technical Institute of Physics and Chemistry (TIPC), Chinese Academy of Sciences, Beijing 100190, China. E-mail: jhhe@mail.ipc.ac.cn
2. School of Chemical & Environmental Engineering, China University of Mining & Technology, Beijing 100083, China
3. Research Institute of Chemical Defense, Beijing 100083, China

Received 15 July 2011; revised 12 December 2011; accepted 14 December 2011

Abstract

Flaky and nanospherical birnessite and birnessite-supported Pt catalysts were successfully prepared and characterized by means of X-ray diffraction (XRD), transmission electron microscopy (TEM), energy dispersive spectroscopy (EDS) and N_2 adsorption-desorption. Effects of the birnessite morphology and Pt reduction method on the catalytic activity for the complete oxidation of formaldehyde (HCHO) were investigated. It was found that flaky birnessite exhibited higher catalytic activity than nanospherical birnessite. The promoting effect of Pt on the birnessite catalyst indicated that the reduction method of the Pt precursor greatly influenced the catalytic performance. Flaky birnessite-supported Pt nanoparticles reduced by KBH_4 showed the highest catalytic activity and could completely oxidize HCHO into CO_2 and H_2O at 50°C, whereas the sample reduced using H_2-plasma showed lower activity for HCHO oxidation. The differences in catalytic activity of these materials were jointly attributed to the effects of pore structure, surface active sites exposed to HCHO and the dispersion of Pt nanoparticles.

Key words: birnessite; manganese oxide; noble metals; formaldehyde oxidation

DOI: 10.1016/S1001-0742(11)60879-6

Introduction

Formaldehyde (HCHO) mainly released from furnishings and decorating materials, is ranked second on the Chinese priority control list of toxic chemicals and is also regarded as one of the predominant indoor pollutants in airtight buildings. As is well known, long-term exposure to indoor air containing HCHO of concentration exceeding its safe limit may cause nasal tumors, respiratory tract irritation, eye membrane irritation and skin irritation (Shen et al., 2008). The World Health Organization also identified HCHO as a carcinogenic and teratogenic chemical. Thus, improving the indoor environment by removing HCHO at low, especially room temperature is of great importance and is attracting increasing attention by researchers. Various methods have been explored to reduce formaldehyde, including physical adsorption with porous materials such as activated carbons, some ceramic materials, zeolites, molecular sieves; chemical reaction with chemical reagents, such as potassium permanganate and organic amines; and catalytic oxidation with metal oxides, such as Ag_2O, PdO, CoO, MnO_2, CeO_2, Mn_3O_4. (Sekine, 2002; Jiao et al., 2006; Srisuda and Virote, 2008; Wen et al., 2011). Among these, physical absorption and chemical reaction are effective for only a short period because of their limited removal capacities.

Heterogeneous catalytic oxidation is considered as one of the most promising technologies for HCHO removal because it can effectively convert HCHO into harmless CO_2 and H_2O at relatively low, even ambient temperature. Conventional catalysts for catalytic oxidation of HCHO are transition metal oxides (Fe_2O_3, MnO_2, CeO_2, and Co_3O_4) (Sekine, 2002), composite oxides (MnO_x-CeO_2, Zn_2SnO_4, MnO_x-SnO_2) (Tang et al., 2006; Wen et al., 2009; Ai et al., 2010), and supported noble metal (Pt, Pd, Rh and Au) catalysts (Zhang et al., 2006, 2009). Among them, the supported noble metal catalysts have been demonstrated to be most effective for HCHO oxidation because of their superior activity at relatively low temperatures. For instance, Álvarez-Galván et al. (2004) found that 0.4 wt.% Pd-Mn/Al_2O_3 with 18.2 wt.% manganese loading could reach complete HCHO combustion at about 90°C. Tang et al. (2006, 2008) investigated MnO_x-CeO_2-supported Ag and Pt catalysts for complete oxidation of HCHO, and found that Ag and Pt enhanced the effective activation of oxygen molecules on the support, which reduced the complete oxidization temperature to 100°C and ambient temperature, respectively. In addition, Zhang and He (2007) reported that TiO_2-supported Pt, with which HCHO could be completely oxidized into

* Corresponding author. E-mail: jhhe@mail.ipc.ac.cn

CO_2 and H_2O at ambient temperature, exhibited superior catalytic performance to TiO_2-supported Au, Rh and Pd. Zhang et al. (2009) also reported that three-dimensionally ordered microporous (3DOM) Au/CeO_2 catalysts with controlled pore sizes showed high catalytic activity with 100% HCHO conversion at 75°C. It should be noted that some transition metal oxides, such as manganese oxides, showed catalytic activities as high as or slightly higher than those of the supported noble metals for complete oxidation of HCHO (Imamura et al., 1994; Lahousse et al., 1998; Sekine and Nishimura, 2001). Our previous works revealed that cryptomelane and birnessite manganese oxides show significantly high catalytic activity, and can completely decompose HCHO into CO_2 and H_2O at very low temperatures (Chen et al., 2007; Tian et al., 2011).

Birnessite is a naturally-occurring manganese oxide, and is widely distributed in soils, sediments and ocean manganese nodules. It has a two-dimensional layered structure consisting of edge-shared MnO_6 octahedra with water molecules and alkali-metal cations in the interlayer region. The interlayer spacing is about 0.7 nm. Birnessite is a non-stoichiometric and poorly crystallized form of manganese dioxide with a general formula of $A_xMnO_{2+y}(H_2O)_z$, in which A represents an alkali cation (Feng et al., 2000). Because of its special physical and chemical properties, birnessite has attracted significant interest for potential applications such as adsorption (Peacock and Sherman, 2007; Chen and He, 2008), ion-exchange (Kim et al., 2007), battery electrodes (Nakayama et al., 2008), electrochemical materials (Yu et al., 2010), magnetic materials (Zhu et al., 2008), and catalysts (Rao et al., 2008; Atribak et al., 2010). It has been demonstrated that birnessite has high catalytic activity for N-demethylation oxidation and degradation of Methylene Blue (Zaied et al., 2011), acetone oxidation (Frías et al., 2007), and complete oxidation of HCHO (Chen et al., 2007). It is conceivable that the decoration of noble metal (such as Ag, Pt, Pd and Au) nanoparticles on birnessite would enhance its catalytic activity for HCHO oxidation. Some works have been carried out to modify birnessite for varied applications by doping different cations into the layer structure (Cai and Suib, 2001; Liu et al., 2011). To the best of our knowledge, however, birnessite-supported noble metal nanoparticles and their application as catalysts for HCHO oxidation have not yet been reported.

In the present study, novel birnessite catalysts were developed by loading with Pt nanoparticles. The effects of birnessite morphology and Pt reduction methods on their catalytic activities were investigated.

1 Experimental

1.1 Catalyst preparation

All chemicals were of analytical grade from Beijing Chemical Works, China and were used without further purification. Flaky and nanospherical birnessite were synthesized via a simple soft chemistry route at room temperature, which is also called "Baeyer test for unsaturation" (Chen et al., 2007).

In a typical preparation of flaky birnessite (designed as Bir(F)), 6.0 g of $KMnO_4$ was dissolved in 400 mL of distilled water, and the mixture was rapidly stirred with a rotational speed of 1200 r/min for about 30 min. A total of 8.0 mL of oleic acid was added dropwise, and an emulsion was formed. After the emulsion was maintained at room temperature for 24 hr, a brown-black product was collected, and washed several times with distilled water and ethanol to remove the residual reactants. Finally, the product was dried at 60°C for 24 hr.

Preparation of nanospherical birnessite (designed as Bir(N)) was almost the same as that of flaky birnessite, except for the amounts of $KMnO_4$, distilled water and oleic acid used, which were 3.0 g, 200 mL and 4 mL, respectively, and the stirring speed of 2400 r/min.

Birnessite-supported 0.8 wt.% Pt catalysts were prepared by the impregnation method. Birnessite was immersed in an ethanol solution of H_2PtCl_6 for 4 hr. The excess ethanol was removed by drying at 60°C for 24 hr. The resultant sample was reduced by two different methods. (a) H_2-plasma reduction: the sample was spread evenly in a Petri dish, and treated in a Plasma Cleaner by H_2 plasma three times for 5 min each. The H_2 flow rate and plasma power were 100 mL/min and 160 W (800 V/200 mA), respectively. The catalyst obtained was designed as Pt/Bir-P. (b) KBH_4 reduction: the sample was added into 40 mL of ethanol under vigorous stirring at 0°C. Then aqueous KBH_4 was added dropwise till the mole ratio of KBH_4 and noble metal was 20:1. After stirring for 4 hr, the mixture was filtered, washed with distilled water and ethanol, and dried at 60°C for 24 hr. The catalyst thus obtained was labeled as Pt/Bir-B.

1.2 Catalyst characterization

X-ray diffraction (XRD) patterns of the samples were performed on a Bruker D8 Focus X-ray diffractometer using Cu $K\alpha$ radiation (40 mA, 40 kV). The data were collected at a scanning rate of 0.1 sec/step over a 2θ range from 10–80°. Transmission electron microscopy (TEM) and energy dispersive spectroscopy (EDS) measurements were recorded on a JEOL JEM-2100F transmission electron microscope. A typical TEM specimen was prepared by ultrasonically suspending catalyst powder in ethanol followed by adding several droplets of the suspension onto a carbon-coated Cu-grid. N_2 adsorption-desorption measurements were performed at 77 K using a Quadrasorb SI automated surface area and pore size analyzer. The as-prepared products were first dried at 100°C before analysis. Specific surface areas were calculated by the Brunauer-Emmett-Teller (BET) method and the average pore sizes were estimated from the adsorption branch of the isotherm by the Barrett-Joyner-Halenda (BJH) formula.

1.3 Catalytic activity measurements

Catalytic activities of all the samples for HCHO oxidation were measured in a fixed-bed reactor under atmospheric pressure. The catalyst (100 mg, 40–60 mesh) was loaded in a quartz tube reactor with a diameter of 4 mm. Gaseous

HCHO was generated by passing a purified air flow over a HCHO-saturated solution in an incubator kept at 0°C, leading to a typical feed gas composition of 460 ppm HCHO. The total flow rate was 50 mL/min in a space velocity of GHSV = 30,000 mL/(g·hr). Effluents from the reactor were analyzed with an on-line Agilent 6890 gas chromatograph using Propaek-Q as the separation column equipped with a FID and Ni catalyst converter, which was used for converting carbon oxides quantitatively into methane in the presence of hydrogen before the detector.No other carbon-containing compounds except CO_2 in the products were detected for the tested catalysts. Thus, HCHO conversion (R_{HCHO}, %) is expressed by the yield of CO_2, and calculated as follows:

$$R_{HCHO} = Y_{CO_2} = \frac{C_{CO_{2\text{-out}}}}{C_{HCHO\text{-in}}} \times 100 \quad (1)$$

where, Y_{CO_2} (%) is the CO_2 yield, $C_{CO_2\text{-out}}$ (vol.%) is the CO_2 concentration in the products, and $C_{HCHO\text{-in}}$ (vol.%) is the HCHO concentration in the feed gas.

2 Results and discussion

2.1 Catalyst preparation and characterization

The results of our previous works indicated that reaction conditions, such as the reactant molar ratio, the volume ratio of oleic acid to water and the reaction temperature, greatly affect the structure and morphology of birnessite (Chen et al., 2007; Zhu and He, 2010; Zhou et al., 2011). Here we changed the stirring speed to obtain a novel birnessite material. Meanwhile, the synthesized materials were decorated by Pt nanoparticles by impregnation. All the samples were characterized by XRD, TEM, EDS and N_2 adsorption-desorption.

Figure 1 shows powder XRD patterns of birnessite samples and birnessite-supported Pt samples. The data indicate that all the samples of Bir(F), Bir(N), Pt/Bir(F)-P and Pt/Bir(F)-B have similar patterns. The diffraction peaks recorded at 2θ of 12.29, 24.33, 36.60, and 65.67° can be well-assigned to the (001), (002), (100), and (110) planes of birnessite, respectively (Chen et al., 2007). The broad and weak peaks indicate the poor crystallinity of the birnessite samples. Both birnessite-supported Pt samples reduced respectively by H_2-plasma and KBH_4 have diffraction peaks similar to those of the corresponding undecorated birnessite samples. There are no significant changes in the XRD peak intensities and line widths. This shows that the loading of Pt did not change the crystalline phase of birnessite. In addition, no diffraction peaks of Pt could be observed, indicating that Pt must be highly dispersed on the birnessite material.

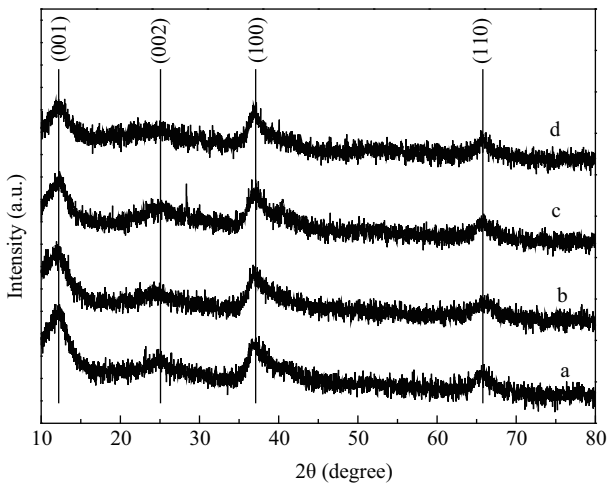

Fig. 1 XRD patterns of birnessite samples and birnessite-supported noble metal samples. (line a) Bir(F); (line b) Bir(N); (line c) Pt/Bir(F)-P; (line d) Pt/Bir(F)-B.

The morphology of the birnessite samples was investigated by TEM, and is shown in Fig. 2. When the stirring speed of the sample preparation is lower (1200 r/min), a flaky material is formed, which consists of nanoplatelets with lengths of 50–90 nm. The increase in the stirring speed leads to the formation of a nanospherical morphology of birnessite. The nanospheres with an average diameter of ca. 130 nm could have been formed by the self-assembly of nanoplatelets as previously observed by our group (Chen et al., 2007). Based on the previous results, in the process of birnessite preparation, oleic acid forms a stable O/W emulsion. In the emulsion, the "Baeyer test for unsaturation" reaction occurs between $KMnO_4$ and oleic acid at the O/W interface and produces birnessite nanoplatelets there. At lower stirring speed, the diameters of emulsion droplets are comparatively large, and the shell formed by lamellar birnessite platelets is loosely packed and unstable, and thus the removal of oleic acid and its residual reactants by ethanol results in collapse of the shell and falling into pieces, giving a flaky morphology. In contrast, smaller droplet oleic acid emulsions are created at the higher stirring speed, and a robust shell is formed by the lamellar birnessite platelets. After reaction, the oleic acid is almost consumed and the core of the shells becomes very small. Therefore, a nanospherical morphology of birnessite is formed after removal of oleic acid and organic residual reactants.

Figures 3a and c display typical TEM images of the flaky birnessite-supported Pt reduced by H_2-plasma and KBH_4, respectively. Clearly, the morphologies remained unchanged (flaky) after the loading of Pt. The corresponding EDS results shown in Fig. 4 reveal the presence of elemental Pt, which indicates that Pt had been loaded successfully on the birnessite material in both cases. Such Pt species produced by H_2-plasma and KBH_4 reduction had been confirmed previously to exist as Pt metallic nanoparticles (He et al., 2002, 2003). As seen from Fig. 3b and d, the Pt nanoparticles of Pt/Bir(F)-B reduced by KBH_4 are much smaller and have a higher degree of dispersion than those of Pt/Bir(F)-P reduced by H_2-plasma. The mean sizes of Pt metal nanoparticles are ca. 2.2 nm and ca. 4.9 nm for Pt/Bir(F)-B and Pt/Bir(F)-P, respectively.

The N_2 adsorption-desorption isotherms and pore size distribution curves of the birnessite samples are shown in Fig. 5. It is indicated from Fig. 5a that all the samples exhibit type II isotherms with type H3 hysteresis loops in the relative pressure range of 0.4–1.0 (Chen et al., 2002; Ding et al., 2005), suggesting the existence of micropore

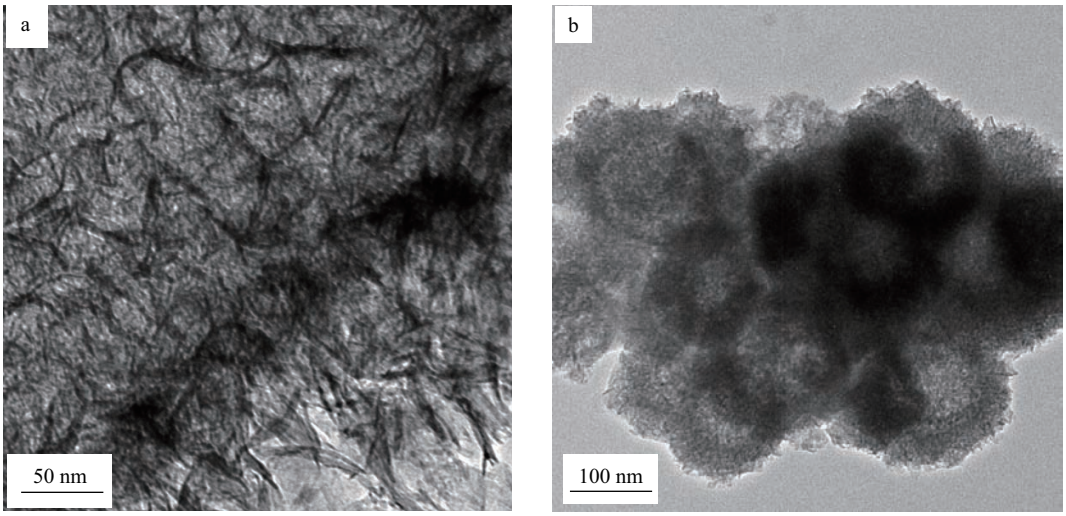

Fig. 2 TEM images of birnessite samples. (a) Bir(F); (b) Bir(N).

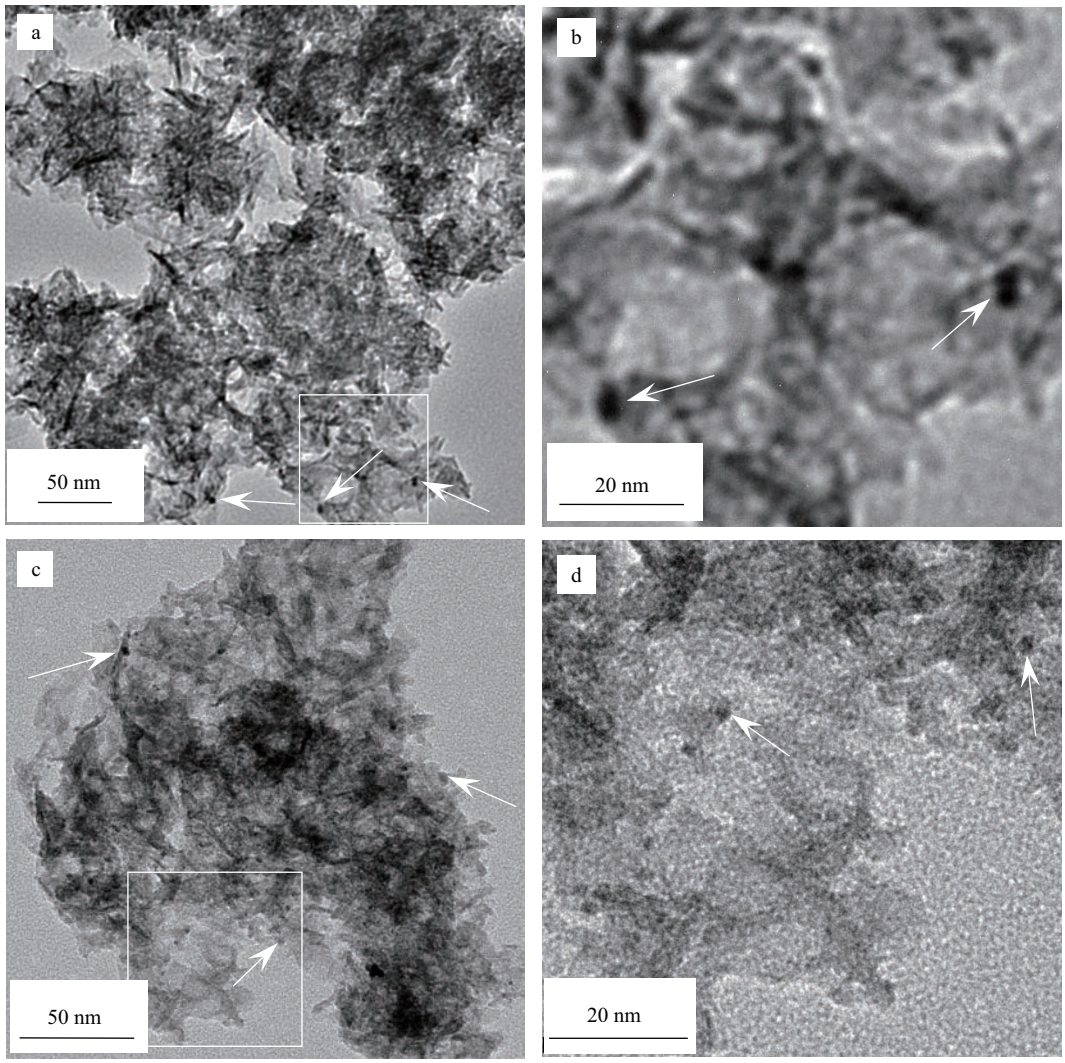

Fig. 3 TEM images of birnessite-supported noble metal samples. (a) Pt/Bir(F)-P; (c) Pt/Bir(F)-B. (b) and (d) are magnified images of the highlighted areas in (a) and (c), respectively. Arrows point to nanoparticles.

filling slit-shaped mesopores with nonuniform shapes or sizes, probably due to the aggregation of nanoparticles. Among these samples, Pt/Bir(F)-B adsorbs apparently more nitrogen molecules than the others, indicating its larger pore volume (as seen in Table 1). Figure 5b shows the pore size distributions of the birnessite samples. The broad primary pore size distribution peaks indicate the nonuniform pores of these materials. The Bir(N) sample has just one primary pore diameter while the other flaky birnessite materials have two primary pore diameters of

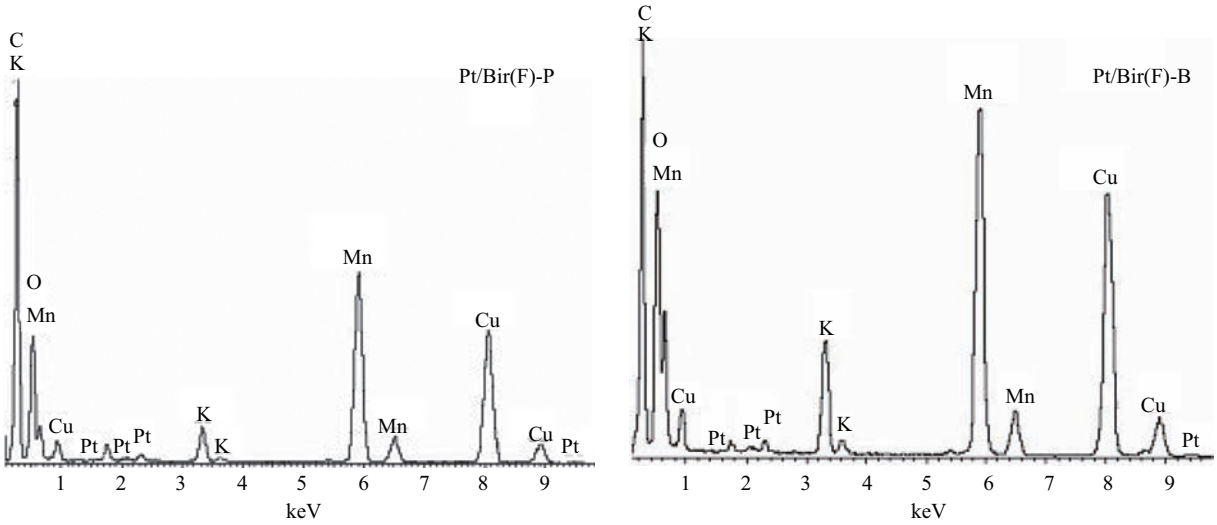

Fig. 4 EDS analyses of as-prepared birnessite-supported Pt samples.

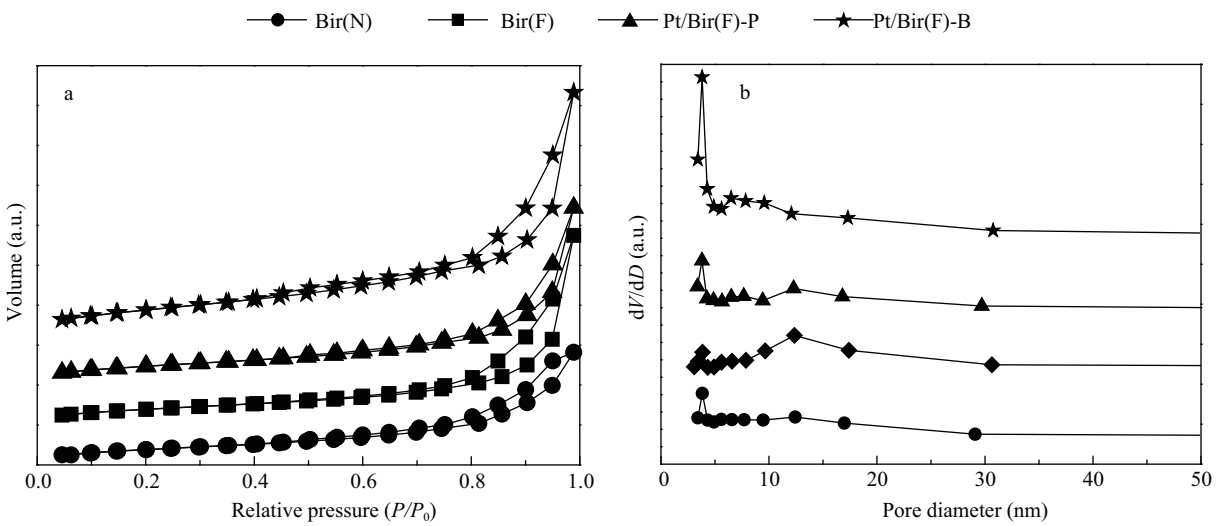

Fig. 5 Nitrogen adsorption-desorption isotherms (a) and pore size distribution curves (b) of the birnessite and birnessite-supported Pt samples.

Table 1 Textural properties of the birnessite samples and birnessite-supported noble metal samples

Catalyst	Surface area (m^2/g)	Pore volume (cm^3/g)	Average pore diameter (nm)
Bir(N)	72.1	0.22	12.1
Bir(F)	74.7	0.37	19.7
Pt/Bir(F)-P	87.3	0.34	15.7
Pt/Bir(F)-B	158.9	0.49	12.3

ca. 1.9 and 6.1 nm. The pore size distribution peaks at 1.9 nm are probably attributable to the textural mesopores on the flakes, and the peak at 6.1 nm may be due to the aggregation of flaky nanomaterials.

Table 1 shows the specific surface area, pore volume and average pore diameter of all the samples. Compared to Bir(N), Bir(F) has slightly higher specific surface area, pore volume and lower average pore diameter. The loading of Pt leads to the increasing of specific surface areas and the decreasing of average pore diameters. Pt/Bir(F)-B has the highest surface area of 158.9 m^2/g and the smallest average pore diameter of 12.3 nm. The pore volume of Pt/Bir(F)-B at 0.49 cm^3/g is also the largest. These results might be due to the occurrence of delamination during the reduction in the KBH_4 solution and subsequent rearrangement of birnessite materials. The higher specific surface area and pore volume of Pt/Bir(F)-B than that of Pt/Bir(F)-P may expose more catalytically active sites of birnessite samples and increase the catalytic activity for HCHO oxidation.

2.2 Catalytic oxidation of HCHO

2.2.1 Effect of the morphology of birnessite

The catalytic activities of flaky and nanospherical birnessite catalysts were evaluated for HCHO oxidation, as shown in Fig. 6. Different from the investigations of catalyst performance in HCHO conversion in many previous works (Sekine, 2002; Chen et al., 2007; Wang et al., 2009), here the activity is expressed as the yield of CO_2 produced during the complete oxidation of HCHO, which can avoid the effects of HCHO polymerization in the solution and adsorption of HCHO on the catalyst surface on its conversion, and describe the performance of HCHO oxidation into CO_2 and H_2O more accurately. Figure 6 shows that at temperatures lower than 80°C, the CO_2

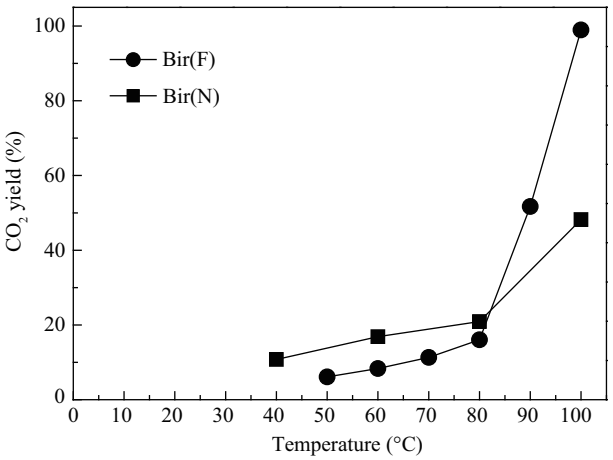

Fig. 6 Effects of the birnessite morphology on the catalytic oxidation of formaldehyde.

yield was quite low, less than 20% over both flaky and nanospherical birnessite. The nanospherical birnessite had slightly higher catalytic activity than the flaky birnessite. With the increase of the reaction temperature to 100°C, however, HCHO was eliminated rapidly over the flaky birnessite, and the CO_2 yield was enhanced up to 100%, greatly higher than that over the nanospherical birnessite (48%). This result may be ascribed to the more easily accessible structure and larger surface area of the flaky birnessite catalyst that exposes more catalytically active sites to HCHO molecules compared to the nanospherical birnessite catalyst. In addition, the larger pore volume of Bir(F) (0.37 cm^3/g) than Bir(N) (0.22 cm^3/g) (Table 1) may also enhance the adsorption and catalytic oxidation of HCHO molecules.

2.2.2 Effect of reduction method

The catalytic activities of flaky birnessite-supported Pt catalysts reduced respectively by H_2-plasma and KBH_4 were also evaluated for HCHO oxidation, as shown in Fig. 7. Compared with the pure flaky birnessite, the loading of Pt improved its catalytic activity for HCHO oxidation. The initial oxidation temperature for the pure flaky birnessite was 50°C, with the complete oxidation of HCHO at 100°C. After the loading of Pt reduced by H_2-plasma, the initial temperature decreased to 40°C, but the temperature for total HCHO oxidation remained unchanged. Comparing these two catalysts, the birnessite-supported Pt reduced by KBH_4 showed superior catalytic activity. The complete oxidation temperature of Pt/Bir(F)-B fell sharply to 50°C. Moreover, even at 20°C, 28% of 460 ppm HCHO could be completely decomposed into CO_2 and H_2O. In comparison with other catalysts reported elsewhere, the current catalysts perform much better in HCHO oxidation under similar conditions. To the best of our knowledge, Pt/SiO_2, $Pt/Ce_{0.8}Zr_{0.2}O_2$, and $Pt/Ce_{0.2}Zr_{0.8}O_2$ only give HCHO conversion of less than 10% at room temperature, and cannot reach 100% even at 120°C (Peng and Wang, 2007).

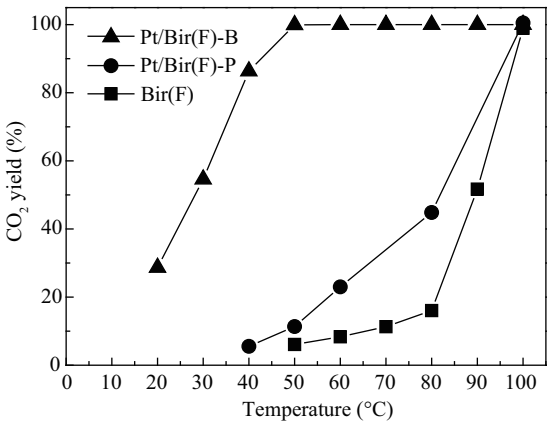

Fig. 7 Effects of reduction methods of birnessite-supported Pt on the catalytic oxidation of formaldehyde.

It is known that the catalytic activity of catalysts for HCHO oxidation is influenced by a combination of factors including surface area, pore structure and the dispersion of noble metals on supports (Chen et al., 2007; Tang et al., 2008). Table 1 indicates that Pt/Bir(F)-B exhibited the highest surface area and pore volume. The adsorption ability of Pt/Bir(F)-B (Fig. 5a) was also higher than that of Pt/Bir(F)-P. All these factors contribute to its higher catalytic activity. Besides, as shown in Fig. 3a–d, the Pt/Bir(F)-B catalyst has Pt nanoparticles of better dispersion and smaller sizes than Pt/Bir(F)-P, which may significantly increase the contact probability between HCHO molecules and Pt nanoparticles, leading to higher catalytic activity for the Pt/Bir(F)-B catalyst than for Pt/Bir(F)-P in HCHO oxidation.

3 Conclusions

In this work, birnessite and birnessite-supported Pt catalysts were successfully prepared. The morphology of the as-prepared birnessite depends strongly on the reaction conditions. Flaky birnessite obtained at lower stirring speed showed higher activity in HCHO oxidation than nanospherical birnessite synthesized at higher stirring speed. The loading of Pt improved the catalytic activity of birnessite. The reduction method of the noble metal loading was found to greatly affect the catalyst performance towards HCHO oxidation. Birnessite-supported Pt reduced by KBH_4 with higher specific surface area, pore volume and better dispersion of Pt nanoparticles exhibited much higher catalytic activity than that reduced by H_2-plasma. 460 ppm HCHO could be rapidly and completely converted into CO_2 and H_2O over Pt/Bir(F)-B even at 50°C.

Acknowledgements

This work was supported by the National Natural Science Foundation of China (No. 20871118, 21007076), the Knowledge Innovation Program of the Chinese Academy of Sciences (CAS) (No. KSCX2-YW-G-059), the National Basic Research Program (973) of China (No. 2010CB934103), and the "Hundred Talents Program" of CAS.

References

Ai Z H, Lee S C, Huang Y, Ho W K, Zhang L Z, 2010. Photocatalytic removal of NO and HCHO over nanocrystalline Zn_2SnO_4 microcubes for indoor air purification. *Journal of Hazardous Materials*, 19(1-3): 141–150.

Álvarez-Galván M C, Pawelec B, de la Peña O'Shea V A, Fierro J L G, Arias P L, 2004. Formaldehyde/methanol combustion on alumina-supported manganese-palladium oxide catalyst. *Applied Catalysis B: Environmental*, 51(2): 83–91.

Atribak I, Bueno-López A, García-García A, Navarro P, Frías D, Montes M, 2010. Catalytic activity for soot combustion of birnessite and cryptomelane. *Applied Catalysis B: Environmental*, 93(3-4): 267–273.

Cai J, Suib S L, 2001. Preparation of layer structure birnessite by air oxidation: synthetic factors and framework dopant effects. *Inorganic Chemistry Communications*, 4(9): 493–495.

Chen H M, He J H, Zhang C B, He H, 2007. Self-assembly of novel mesoporous manganese oxide nanostructures and their application in oxidative decomposition of formaldehyde. *Journal of Physical Chemistry C*, 111(49): 18033–18038.

Chen H M, He J H, 2008. Facile synthesis of monodisperse manganese oxide nanostructures and their application in water treatment. *Journal of Physical Chemistry C*, 112(45): 17540–17545.

Chen X, Shen Y F, Suib S L, O'Young C L, 2002. Characterization of manganese oxide octahedral molecular sieve (M-OMS-2) materials with different metal cation dopants. *Chemistry of Materials*, 14(2): 940–948.

Ding Y S, Shen X F, Sithambaram S, Gomez S, Kumar R, Crisostomo V M B et al., 2005. Synthesis and catalytic activity of cryptomelane-type manganese dioxide nanomaterials produced by a novel solvent-free method. *Chemistry of Materials*, 17(21): 5382–5389.

Feng Q, Liu L, Yanagisawa K, 2000. Effects of synthesis parameters on the formation of birnessite-type manganese oxides. *Journal of Materials Science Letters*, 19(17): 1567–1570.

Frías D, Nousir S, Barrio I, Montes M, López T, Centeno M A et al., 2007. Synthesis and characterization of cryptomelane- and birnessite-type oxides: Precursor effect. *Materials Characterization*, 58(8-9): 776–781.

He J H, Ichinose I, Kunitake T, Nakao A, 2002. In situ synthesis of noble metal nanoparticles in ultrathin TiO_2-Gel films by a combination of ion-exchange and reduction processes. *Langmuir*, 18(25): 10005–10010.

He J H, Kunitake T, Nakao A, 2003. Facile in situ synthesis of noble metal nanoparticles in porous cellulose fibers. *Chemistry of Materials*, 15(23): 4401–4406.

Imamura S, Uchihori D, Utani K, Ito T, 1994. Oxidative decomposition of formaldehyde on silver-cerium composite oxide catalyst. *Catalysis Letters*, 24(3-4): 377–384.

Jiao Z, Luo P C, Wu Y T, Ding S, Zhang Z B, 2006. Absorption of lean formaldehyde from air with Na_2SO_3 solution. *Journal of Hazardous Materials*, 134(1-3): 176–182.

Kim Y, Hong Y, Kim M G, Cho J, 2007. $Li_{0.93}[Li_{0.21}Co_{0.28}Mn_{0.51}]O_2$ nanoparticles for lithium battery cathode material made by cationic exchange from K-birnessite. *Electrochemistry Communications*, 9(5): 1041–1046.

Lahousse C, Bernier A, Grange P, Delmon B, Papaefthimiou P, Ioannides T et al., 1998. Evaluation of γ-MnO_2 as a VOC removal catalyst: Comparison with a noble metal catalyst. *Journal of Catalysis*, 178(1): 214–225.

Liu L L, Tian H, He J H, Yang Q W, Wang D, 2011. Progress in cryptomelane- and birnessite-type manganese oxides. *Chemistry*, 74(4): 291–297.

Nakayama M, Kanaya T, Lee J W, Popov B N, 2008. Electrochemical synthesis of birnessite-type layered manganese oxides for rechargeable lithium batteries. *Journal of Power Sources*, 179(1): 361–366.

Peacock C L, Sherman D M, 2007. Sorption of Ni by birnessite: Equilibrium controls on Ni in seawater. *Chemical Geology*, 238(1-2): 94–106.

Peng J X, Wang S D, 2007. Performance and characterization of supported metal catalysts for complete oxidation of formaldehyde at low temperatures. *Applied Catalysis B: Environmental*, 73(3-4): 282–291.

Rao M A, Iamarino G, Scelza R, Russo F, Gianfreda L, 2008. Oxidative transformation of aqueous phenolic mixtures by birnessite-mediated catalysis. *Science of the Total Environment*, 407(1): 438–446.

Sekine Y, Nishimura A, 2001. Removal of formaldehyde from indoor air by passive type air-cleaning materials. *Atmospheric Environment*, 35(11): 2001–2007.

Sekine Y, 2002. Oxidative decomposition of formaldehyde by metal oxides at room temperature. *Atmospheric Environment*, 36(35): 5543–5547.

Shen Y N, Yang X Z, Wang Y Z, Zhang Y B, Zhu H Y, Gao L et al., 2008. The states of gold species in CeO_2 supported gold catalyst for formaldehyde oxidation. *Applied Catalysis B: Environmental*, 79(2): 142–148.

Srisuda S, Virote B, 2008. Adsorption of formaldehyde vapor by amine-functionalized mesoporous silica materials. *Journal of Environmental Sciences*, 20(3): 379–384.

Tang X F, Chen J L, Li Y G, Li Y, Xu Y D, Shen W J, 2006a. Complete oxidation of formaldehyde over Ag/MnO_x-CeO_2 catalysts. *Chemical Engineering Journal*, 118(1-2): 119–125.

Tang X F, Li Y G, Huang X M, Xu Y D, Zhu H Q, Wang J G et al., 2006b. MnO_x-CeO_2 mixed oxide catalysts for complete oxidation of formaldehyde: Effect of preparation method and calcination temperature. *Applied Catalysis B: Environmental*, 62(3-4): 265–273.

Tang X F, Chen J L, Huang X M, Xu Y D, Shen W J, 2008. Pt/MnO_x-CeO_2 catalysts for the complete oxidation of formaldehyde at ambient temperature. *Applied Catalysis B: Environmental*, 81(1-2): 115–121.

Tian H, He J H, Zhang X D, Zhou L, Wang D H, 2011. Facile synthesis of porous manganese oxide K-OMS-2 materials and their catalytic activity for formaldehyde oxidation. *Microporous and Mesoporous Materials*, 138(1-3): 118–122.

Yu P, Zhang X, Chen Y, Ma Y W, 2010. Self-template route to MnO_2 hollow structures for supercapacitors. *Materials Letters*, 64(13): 1480–1482.

Wang L F, Sakurai M, Kameyama H, 2009. Study of catalytic decomposition of formaldehyde on Pt/TiO_2 alumite catalyst at ambient temperature. *Journal of Hazardous Materials*, 167(1-3): 399–405.

Wen Q B, Li C T, Cai Z H, Zhang W, Gao H L, Chen L J et al., 2011. Study on activated carbon derived from sewage sludge for adsorption of gaseous formaldehyde. *Bioresource Technology*, 102(2): 942–947.

Wen Y R, Tang X, Li J H, Hao J M, Wei L S, Tang X F, 2009. Impact of synthesis method on catalytic performance of MnO_x-SnO_2 for controlling formaldehyde emission. *Catal-*

ysis Communications, 10(8): 1157–1160.

Zaied M, Peulon S, Bellakha N, Desmazières B, Chaussé A, 2011. Studies of N-demethylation oxidative and degradation of methylene blue by thin layers of birnessite electrodeposited onto SnO_2. *Applied Catalysis B: Environmental*, 101(3-4): 441–450.

Zhang C B, He H, Tanaka K I, 2006. Catalytic performance and mechanism of a Pt/TiO_2 catalyst for the oxidation of formaldehyde at room temperature. *Applied Catalysis B: Environmental*, 65(1-2): 37–43.

Zhang C B, He H, 2007. A comparative study of TiO_2 supported noble metal catalysts for the oxidation of formaldehyde at room temperature. *Catalysis Today*, 126(3-4): 345–350.

Zhang J, Jin Y, Li C Y, Shen Y N, Han L, Hu Z X et al., 2009. Creation of three-dimensionally ordered macroporous Au/CeO_2 catalysts with controlled pore sizes and their enhanced catalytic performance for formaldehyde oxidation. *Applied Catalysis B: Environmental*, 91(1-2): 11–20.

Zhou L, Hu Y C, He J H, 2011. *In-situ* collapse self-assembly route to synthesize manganese oxide nanostructured materials. *Acta Chimica Sinica*, 69(6): 666–672.

Zhu H T, Luo J, Yang H X, Liang J K, Rao G H, Li J B et al., 2008. Birnessite-type MnO_2 nanowalls and their magnetic properties. *Journal of Physical Chemistry C*, 112(44): 17089–17094.

Zhu J Y, He J H, 2010. Effects of reaction conditions on the structure, morphology and size of manganese oxide nanoparticles. *Acta Chimica Sinica*, 68(10): 961–968.

JOURNAL OF ENVIRONMENTAL SCIENCES

Journal of Environmental Sciences (Established in 1989)
Vol. 24 No. 6 2012

Supervised by	Chinese Academy of Sciences	**Published by**	Science Press, Beijing, China
Sponsored by	Research Center for Eco-Environmental Sciences, Chinese Academy of Sciences		Elsevier Limited, The Netherlands
		Distributed by	
Edited by	Editorial Office of Journal of Environmental Sciences (JES) P. O. Box 2871, Beijing 100085, China Tel: 86-10-62920553; http://www.jesc.ac.cn E-mail: jesc@263.net, jesc@rcees.ac.cn	Domestic	Science Press, 16 Donghuangchenggen North Street, Beijing 100717, China Local Post Offices through China
		Foreign	Elsevier Limited http://www.elsevier.com/locate/jes
Editor-in-chief	Hongxiao Tang	**Printed by**	Beijing Beilin Printing House, 100083, China

CN 11-2629/X **Domestic postcode: 2-580** **Domestic price per issue RMB ¥ 110.00**

ISSN 1001-0742